

Deep Learning Neural Network Approach for Predicting the Sorption of Ionizable and Polar Organic Pollutants to a Wide Range of Carbonaceous Materials

Gabriel Sigmund, Mehdi Gharasoo, Thorsten Hüffer, and Thilo Hofmann*



Cite This: *Environ. Sci. Technol.* 2020, 54, 4583–4591



Read Online

ACCESS |



Metrics & More

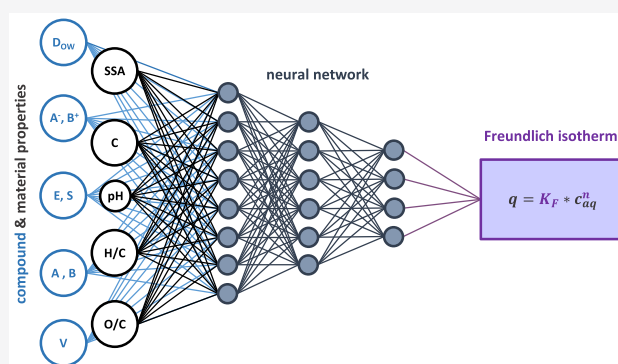


Article Recommendations



Supporting Information

ABSTRACT: Most contaminants of emerging concern are polar and/or ionizable organic compounds, whose removal from engineered and environmental systems is difficult. Carbonaceous sorbents include activated carbon, biochar, fullerenes, and carbon nanotubes, with applications such as drinking water filtration, wastewater treatment, and contaminant remediation. Tools for predicting sorption of many emerging contaminants to these sorbents are lacking because existing models were developed for neutral compounds. A method to select the appropriate sorbent for a given contaminant based on the ability to predict sorption is required by researchers and practitioners alike. Here, we present a widely applicable deep learning neural network approach that excellently predicted the conventionally used Freundlich isotherm fitting parameters $\log K_F$ and n ($R^2 > 0.98$ for $\log K_F$, and $R^2 > 0.91$ for n). The neural network models are based on parameters generally available for carbonaceous sorbents and/or parameters freely available from online databases. A freely accessible graphical user interface is provided.



1. INTRODUCTION

Persistent organic contaminants (POPs) are hydrophobic organic compounds that include the original 12 compounds regulated in the Stockholm convention (the “dirty dozen”). These toxic compounds have been of special concern because of their longevity (“persistence”) and their potential long-range atmospheric transport. Over the past several decades, POPs and their environmental fate have been widely studied and approaches to elucidate their fate in the natural environment have been developed.¹ Today, many contaminants of emerging concern are polar and/or ionizable organic compounds, including pesticides, pharmaceuticals, and personal care products. For example, in 2010, approximately 50% of the industrial chemicals falling under European chemicals regulation (REACH) were ionizable organic compounds; of these, 27% were acids, 14% were bases, and 8% were zwitterions.²

A state-of-the-art approach to predict the sorption of neutral hydrophobic organic contaminants to a given material (sorbent) are poly-parameter linear free-energy relationships (ppLFER).^{3–6} The ppLFER concept for neutral compounds is based on the Abraham parameters E (excess molar refraction), S (dipolarity/polarizability), A (H-bond acidity), B (H-bond basicity), V (McGowan molar volume, $\text{cm}^3 \text{mol}^{-1}/100$), and L (log of the hexadecane–air partition coefficient). In addition, the sorption of organic compounds to carbonaceous sorbents is concentration-dependent (non-linear), a factor that was

recently introduced into ppLFER for predicting the sorption of neutral organic compounds to activated carbon⁴ and to soot.⁵

Carbonaceous sorbent materials, such as activated carbon, soot, biochar, and carbon nanotubes (CNTs), have a wide range of applications, including drinking water filtration systems, wastewater treatment plants, and soil and sediment remediation. There are major limitations to the use of conventional ppLFER in the characterization of these systems. Specifically, the development of each ppLFER requires a substantial number of experiments with a wide range of compounds, such that every model is limited to a single sorbent the ppLFER must be developed for individually. Thus, compared to existing models, the ability to predict contaminant sorption as a function of the properties of the sorbent would be of great advantage, as it would facilitate selection of both the appropriate sorbent and its quantity for a given application.

Moreover, methods developed to predict the sorption of neutral compounds, such as the ppLFER, are not applicable to

Received: October 18, 2019
Revised: February 28, 2020
Accepted: March 2, 2020
Published: March 3, 2020



charged compounds because the occurrence of additional interactions, including electrostatic repulsion and attraction, charge-assisted H-bonding, cation bridging, cation- π bonding, and anion- π bonding, will depend on the speciation/dissociation of a given ionizable organic compound.^{7–10} These interactions cannot be accounted for in existing ppLFFER concepts, and the prediction of the environmental fate of charged compounds is accordingly hindered.

A simple sorbent-dependent model based on experimental data to predict the sorption of organic acids was recently proposed.¹¹ The model predicted sorption distribution coefficients using the pH-dependent lipophilicity parameter $\log D_{OW}$ and the specific surface area (SSA) of the carbonaceous sorbent. However, (i) acids are only one of the three types of ionizable organic compounds; (ii) the model could not satisfactorily predict the literature data likely because of differences in measurement protocols, including the measurement of the SSA,¹² and (iii) the concentration-dependent nonlinearity of sorption was not predicted.

To address these issues, we collected published data from over 10 years of experimental research. As the Freundlich isotherm fitting model, first published in 1907,¹³ was the most widely applied model (66% of 210 papers collected), it was chosen as a target for prediction. To predict the Freundlich fitting parameters for the sorption of ionizable organic compounds to carbonaceous sorbents, a deep learning approach was developed and tested on independent literature data to validate the model's performance. The results showed that this newly developed method is able to predict the sorption of anionic, cationic, and zwitterionic ionizable organic compounds to carbonaceous sorbents and is therefore widely applicable. Moreover, it is based on parameters generally available for carbonaceous sorbents and additional compound descriptors that are freely available from online databases. A freely accessible graphical user interface is provided by the authors.

2. METHODS

2.1. Data Mining from the Literature. The literature from 2005 to 2019 was searched using three-word Scopus searches, including one keyword for the sorbent (CNT, activated carbon, biochar, graphene, carbonaceous, or graphite) and one keyword for the sorbate (polar or ionizable) and "sorption." Reviews and nonrelevant papers were excluded from the database, which resulted in a list of 210 papers. Thereafter, only papers including the Freundlich isotherm fit and reporting the SSA as well as the C, H, and O contents were selected for further analysis, which resulted in a core database sourced from 47 publications.^{11,14–59} Every sorbent-sorbate combination used in these publications received a separate line in the database, which resulted in 328 lines for negatively charged and polar compounds (Table S1 in the Supporting Information) and 139 lines for compounds with a positive charge (Table S2 in the Supporting Information). Each line contained information on the combination of one single sorbate and one single sorbent under one specific pH condition. If pH was not reported, a pH of 7 was assumed for the sorbate property calculations (i.e., $\log D_{OW}$). For highly carbonized materials with a carbon content >90% and no measurable H content, an H content of 0.01% was assumed for H/C calculations. The validity of this approach was tested by running the neural network with and without these data. The predictions based on the smaller data set did not differ

substantially but were associated with larger prediction errors and a smaller working range because of the decreased number of available training items (data not shown).

2.2. Deep Learning Neural Network Setup. The feed-forward neural network was trained using an automated Bayesian regularization technique^{60,61} in which the weights and biases of the network are assumed to be random variables with specified distributions. The regularization parameters are then connected to the variances associated with these distributions and are estimated using statistical techniques. The Bayesian regularization algorithm generally works best when the inputs and outputs are approximately scaled in the range between -1 and 1 . Because K_F values are orders of magnitude greater than this range and change drastically, considering $\log K_F$, instead of K_F , as a target parameter significantly improved the quality of the trainings. To further improve the model, outliers were excluded from the training data sets. To this end, data lines containing n and $\log K_F$ values smaller than the 5th percentile and larger than the 95th percentile were excluded from the training set.

Overfitting is a common problem during neural network training. In an over-fitted neural network, although the error of the training set is driven to a small value, the presentation of new data to the same network can result in large errors. This is because the trained network has memorized only the training examples and has not learned to generalize to new situations. The number of parameters in this study was reasonably smaller than the total number of data in the training set such that the chance of overfitting was small. In addition, network generalization was improved by training the neural network on the same data set multiple (50) times. The same Bayesian regularization back-propagation training technique was used in all multitraining sessions. Each training session started with different initial weights and biases as well as different divisions of data for training (70%), validation (15%), and test (15%) sets. Because different conditions led to different solutions, the final estimations were obtained by averaging between the outputs from all 50 trained networks. As a result, in the majority of cases, the mean squared error for the average output was lower than that for the individual sessions. The employed multitraining technique thus led to a better network generalization, which improved the network forecasting capability. This was particularly helpful for the small and noisy data set of compounds containing a positive charge.

Because the computational costs of multiple training can be high, we implemented a parallel computation scheme to greatly reduce the training times. The computational time for a complete multitraining session on an Intel Core i7-9700K CPU with 32 GB RAM was under a minute using all eight CPU cores.

2.3. Sensitivity Analysis. The variance-based global sensitivity analysis (GSA) of Sobol (2001)⁶² was used to determine the importance of individual input parameters for the outcome of neural network predictions of $\log K_F$ and n . A GSA, in contrast to a local sensitivity analysis (LSA), considers variabilities in the full range of values for all input parameters simultaneously. It is thus superior to LSA, in which the focus is the variability of a single parameter value at a time. As such, GSA offers a more rigorous solution for elucidating the impact of input parameter's variability considering that all other parameters are also variable. We used a latin hypercube sequencing sampler to generate 200,000 sample scenarios that uniformly covered the space of the input parameters. For each

Table 1. Training Range of the Individual Input Parameters for Predicting the Freundlich Parameters $\log K_F$ and n of Negatively Charged and Polar Compounds^a

	C [%]	H/C	O/C	SSA [m ² /g]	pH	log D_{OW}	A [%]	E [cm ³ mol ⁻¹ /100]	S	A	B	V [cm ³ mol ⁻¹ /100]
min	10	0.001	0.0002	1	3.3	-9.64	0.00	0.39	0.57	0.00	0.15	0.61
max	98	2.883	1.2002	1100	11.8	5.74	100.00	3.50	3.60	1.35	3.29	3.10

^aAbbreviations: carbon content (C, %), molar ratios H/C and O/C, specific surface area (SSA, m²/g), abundance of negatively charged species (A^- , %), E (excess molar refraction), S (dipolarity/polarizability), A (H-bond acidity), B (H-bond basicity), and V (molar volume).

Table 2. Training Range of the Individual Input Parameters for Predicting the Freundlich Parameters $\log K_F$ and n of Cations and Zwitterions^a

	C [%]	H/C	O/C	SSA [m ² /g]	pH	log D_{OW}	A^- [%]	B^+ [%]	E [cm ³ mol ⁻¹ /100]	S	A	B	V [cm ³ mol ⁻¹ /100]
min	20	0.001	0.0002	1	3.0	-8.55	0	0.001	0.63	0.84	0.00	0.25	0.68
max	99	1.808	0.8882	2000	10.0	9.50	100	100	3.50	4.07	1.65	6.52	7.04

^aAbbreviations: carbon content (C, %), molar ratios H/C and O/C, SSA (m²/g), abundance of negatively charged species (A^- , %), abundance of positively charged species (B^+ , %), E (excess molar refraction), S (dipolarity/polarizability), A (H-bond acidity), B (H-bond basicity), and V (molar volume).

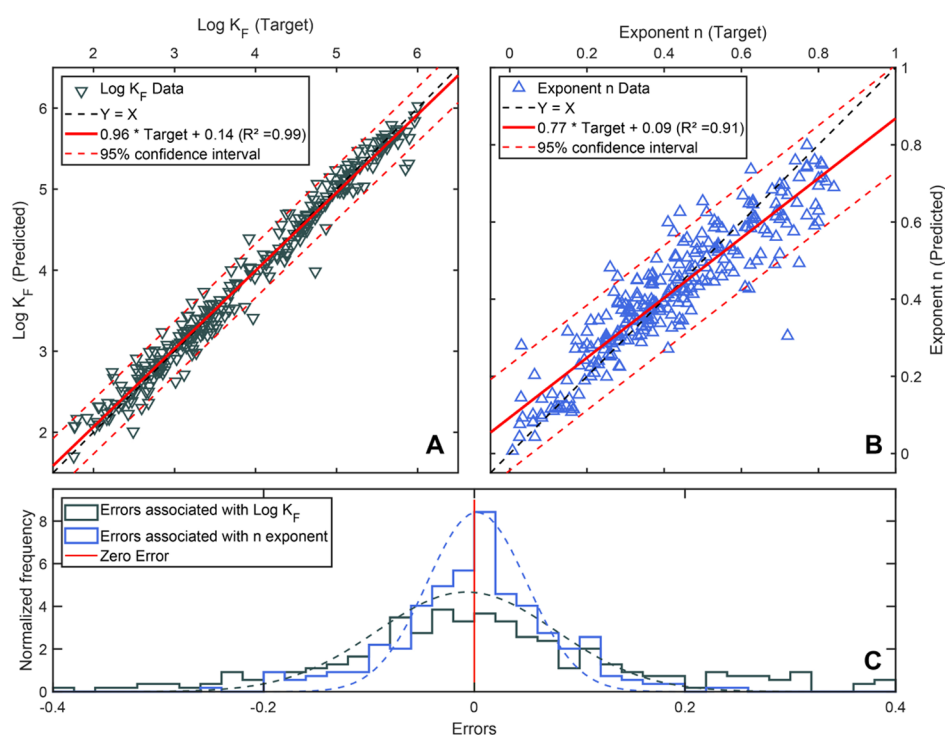


Figure 1. Measured Freundlich parameters $\log K_F$ and $t-n$ (“target”) from the training set of polar and negatively charged compounds plotted against $\log K_F$ and n , as predicted by the neural network model. (A) Shows the model for $\log K_F$ (grey ∇) and the 95% confidence interval for the prediction (dashed red lines). (B) Shows the model for the exponent n (blue Δ) and the 95% confidence interval for the prediction (dashed red lines). (C) Shows the normalized error frequency associated with the predictions of K_F and n (sample size = 313).

realization, input variables were perturbed at random within the range of each parameter variability in the full training data set. The fully trained model was solved 200,000 times for each randomly generated realization, for which the abovementioned computational setup took about 20 min. The spatial variability of each input parameter was assumed to follow a normal distribution defined by the standard deviation and mean value of that parameter alone; no correlation was assumed between the spatial variabilities of different input parameters. The first-order Sobol indices (S_i) were then calculated from the GSA, as described in Gharasoo et al. (2019)⁶³ and in Sobol and Levitan (1999).⁶⁴

2.4. Graphical User Interface. To maximize their range of applicability, the models for the graphical user interface were

built on the complete data set (including the data lines previously excluded for validation). The interface is conceptually similar to previously developed graphical user interfaces.^{65,66} The “CFrePred” graphical user interface is capable of importing and exporting data from/to Excel or Open Office to ease data transfer to the widely used file format “.xls”.

3. RESULTS AND DISCUSSION

3.1. Selection of Parameters. The classical presentation of the Freundlich equation is

$$q = K_F \times c_{aq}^n \quad (1)$$

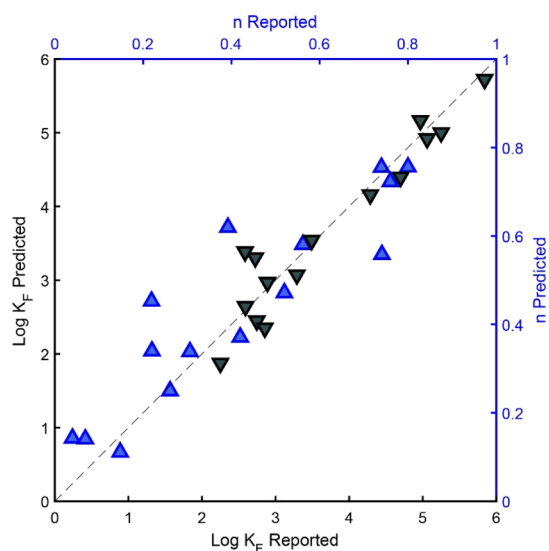


Figure 2. Measured Freundlich fit parameters $\log K_F$ (grey ▼) and n (blue ▲) from the independent data set for negatively charged and polar compounds plotted against parameters predicted by the neural network model (sample size = 15).

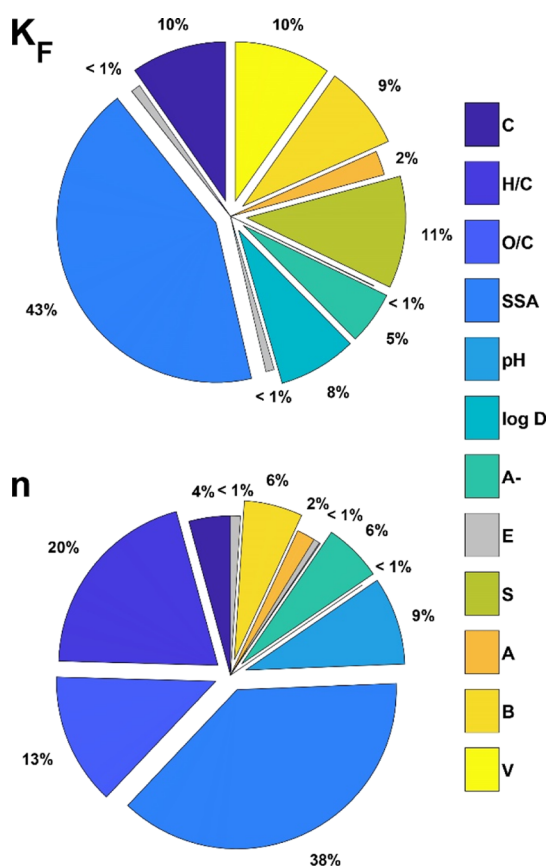


Figure 3. GSA first-order indices (Si) for the prediction of the Freundlich parameters for negatively charged and polar compounds. Abbreviations: carbon content (C, %), molar ratios H/C and O/C, SSA (m^2/g), and abundance of ionized negatively charged species (A^- , %), E (excess molar refraction), S (dipolarity/polarizability), A (H-bond acidity), B (H-bond basicity), and V (molar volume).

where q [$\mu\text{g}/\text{kg}$] describes sorbate loading onto the sorbent, c_{aq} [$\mu\text{g}/\text{L}$] is the aqueous concentration of the sorbate, K_F

[$\frac{\mu\text{g}/\text{kg}}{(\mu\text{g}/\text{L})^n}$] is the Freundlich constant, and n [-] is the Freundlich exponent representing isotherm nonlinearity. The units of K_F change as a function of the units used for q and c_{aq} . Several researchers have reported K_F without units and/or “ $1/n$ ” instead of “ n ”, such that care must be taken when comparing literature data. For this study, the Freundlich parameters K_F and n sourced from the literature were transformed to the form shown here and defined as the target parameters for prediction.

Four sorbent property parameters commonly reported in the literature and previously linked to sorption behavior were selected.^{7,11,54,67,68} The sorbent content of carbon (C, %), hydrogen (H, %), and oxygen (O, %) as well as the SSA (m^2/g) were sourced from the literature, and the molar ratios H/C and O/C were calculated. Among the >200 screened publications,^{11,14–59} 47 reported all of the above parameters. In addition, pH was also used as a fifth parameter. Thereby, for a given material, C is a proxy for homogeneity, SSA is a proxy for porosity and accessible sorption sites, H/C is a proxy for aromaticity, and O/C is a proxy for polarity, and the experimental pH is linked to the material’s surface charge (negative charge increasing with pH).

Eight sorbate properties were selected to describe the molecular properties of ionizable and polar compounds: The five Abraham solute parameters (E , S , A , B , and V) were obtained from the freely accessible UFZ-LSER database.⁶⁹ The sixth Abraham parameter, describing hexadecane–air distribution (L), was not used because a pH-independent hydrophobicity parameter is conceptually not applicable to ionizable organic compounds, which dissociate depending on the surrounding pH and whose hydrophobicity thereby changes. Instead of L , the pH-dependent hydrophobicity parameter $\log D_{\text{OW}}$ was calculated at the experimental pH, using the freely accessible ChemAxon online platform (chemicalize.com). When P (octanol–water partition coefficient for the neutral species) and P_i (octanol–water partition coefficient for the ionized species) are known, D_{ow} for acidic (anionic) compounds can be calculated as

$$D_{\text{OW}} = \frac{P + P_i \times 10^{\text{pH}-\text{p}K_a}}{1 + 10^{\text{pH}-\text{p}K_a}} \quad (2)$$

and D_{ow} for basic (cationic) compounds can be calculated as

$$D_{\text{OW}} = \frac{P + P_i \times 10^{\text{p}K_a-\text{pH}}}{1 + 10^{\text{p}K_a-\text{pH}}} \quad (3)$$

In addition, we used the experimental pH and the dissociation constants of the ionizable organic compounds to calculate the abundance of ionized species present under a given condition using the Henderson–Hasselbach equation.

Several attempts to train the neural network for all types of compounds combined were not able to obtain meaningful results (data not shown), most likely because compounds containing a positive charge behave differently from polar and anionic compounds. For example, the hydrophobicity of acidic and polar compounds is generally positively linked to sorption. As the hydrophobicity of acidic compounds decreases with dissociation, sorption decreases as well. This can be explained in part by the electrostatic repulsion of the anions from the generally negatively charged surface functional groups on the carbonaceous sorbents. In contrast, when cationic ionizable organic compounds dissociate and their hydrophobicity decreases, their positive charge can be electrostatically

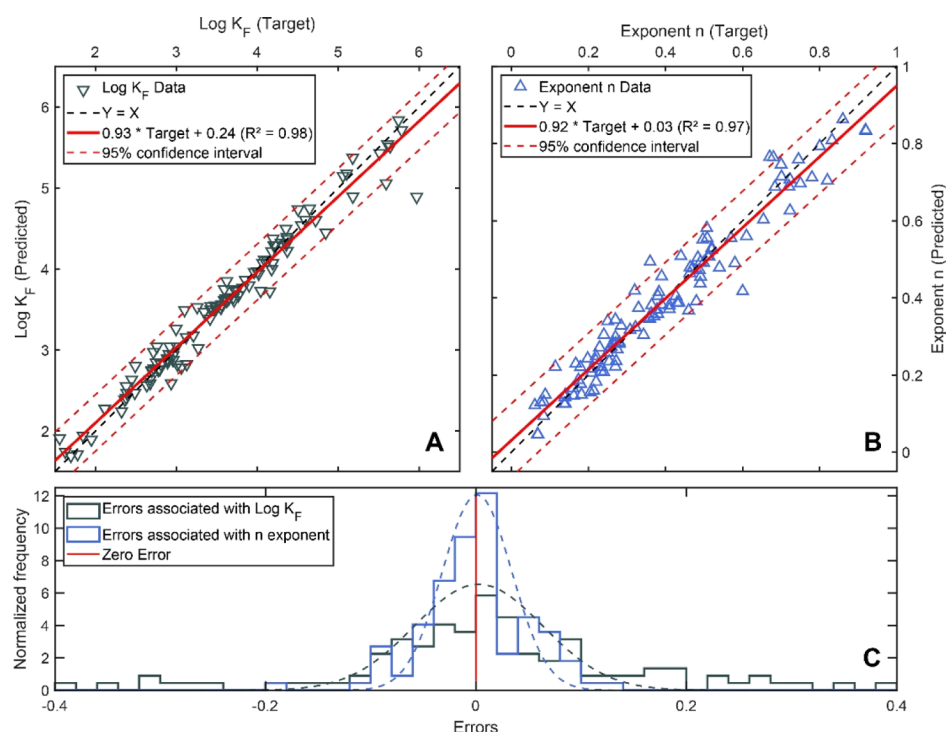


Figure 4. Measured Freundlich fit parameters $\log K_F$ and n (“target”) from the training set of cations and zwitterions plotted against $\log K_F$ and n predicted by the neural network model. (A) Shows the model for $\log K_F$ (∇) and the 95% confidence interval for the prediction (dashed red lines). (B) Shows the model for the exponent n (blue \triangle) and the 95% confidence interval (dashed red lines). (C) Shows the normalized errors associated with the predictions of K_F and n (sample size = 133).

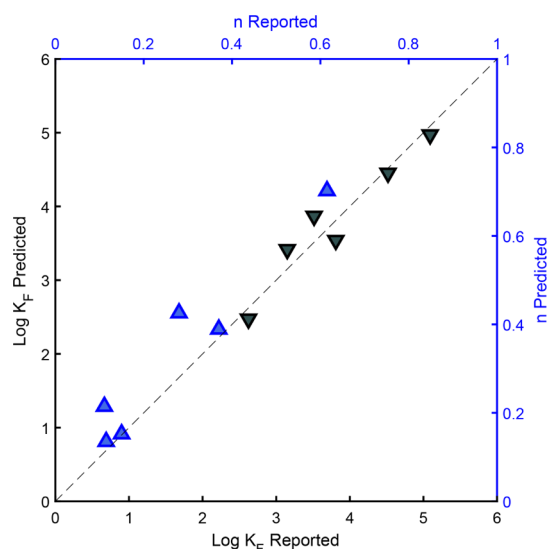


Figure 5. Measured Freundlich fit parameters $\log K_F$ (grey ∇) and n (blue \blacktriangle) from the independent data set for cations and zwitterions plotted against the parameters predicted by the neural network model (sample size = 6).

attractive to the negatively charged functional groups on the sorbent surface, thereby increasing sorption.

We therefore subdivided the data set into (i) negatively charged and polar compounds and (ii) compounds containing a positive charge. Zwitterions, which can have both charges, were grouped according to their speciation, with 0.001% of the compound being positively charged set as the threshold to place the compound in the second group. At <0.001% of the compound being positively charged, the contribution of the

positive charge to overall sorption is most likely negligible. The two databases are presented in searchable xls Tables S1 and S2 of the [Supporting Information](#).

3.2. Predicting Sorption of Anions and Polar Compounds. The model was constructed on the basis of a feed-forward deep learning neural network (also known as a multi-layered network of neurons) with 20 hidden layers between the input and output layers. These hidden layers process the complex nonlinear relationships between the 12 input parameters (sorbent and sorbate descriptors from [Section 3.1](#)) and the two output parameters ($\log K_F$ and n). The neural-network-based predictions of $\log K_F$ and n yielded very accurate predictions of the data from the training set and were able to cover a wide range of input parameters, as shown in [Table 1](#) and [Figure 1](#).

The 95% confidence interval for the prediction of $\log K_F$ shows that predictions of K_F are associated with errors below one order of magnitude. This is in the same or lower range as the errors of state-of-the-art prediction models of single carbonaceous sorbents and neutral compounds,^{4,5} which demonstrated the excellent performance of our model in predicting the $\log K_F$ for polar and anionic compounds as a function of sorbent properties. Typically, for carbonaceous sorbents, the concentration dependence of sorption (non-linearity) increases at high concentrations (i.e., n decreases). Thus, the slightly larger errors associated with the prediction of n ([Figure 1](#)) can partially be explained by the strong dependence of the nonlinearity of sorption on the concentration range of interest during the measurement of a sorption isotherm. The values obtained from the literature were calculated based on widely varying concentration ranges (ng/L range to mg/L range for c_{aq} in the aqueous solution).

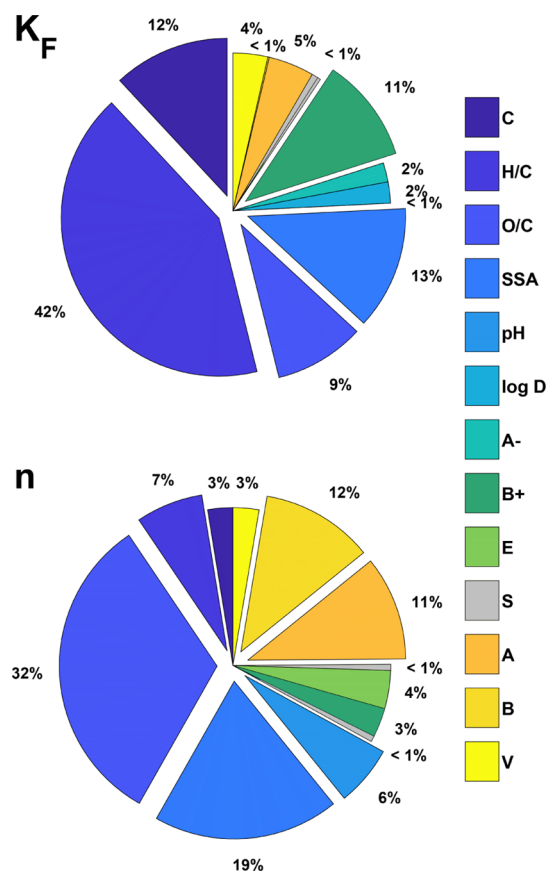


Figure 6. GSA first-order indices (S_i) for the prediction of the Freundlich parameters for cations and zwitterions. Abbreviations: carbon content (C, %), molar ratios H/C and O/C, SSA (m^2/g), amount of ionized negatively charged species (A^- , %), amount of ionized positively charged species (B^+ , %), E (excess molar refraction), S (dipolarity/polarizability), A (H-bond acidity), B (H-bond basicity), and V (molar volume).

Therefore, the performance of the model in predicting the exponent n can be considered to be very good.

To validate the predictions, we randomly excluded 15 data lines (equal to 5% of the total dataset, see Table S3 in the Supporting Information) from the training data set prior to neural network training. The prediction results for these independent data are shown in Figure 2 and confirm the good model performance obtained for the K_F and n of negatively charged and polar compounds.

The variance-based GSA of Sobol (2001)⁶² was used to determine the importance of individual input parameters for the outcome of the neural network predictions of $\log K_F$ and n . The first-order Sobol indices for the global sensitivity of $\log K_F$ and n to the 12 input parameters are displayed in Figure 3. The SSA, the sorbent aromaticity, and polarity as approximated by H/C and O/C were the most important sorbent parameters for the prediction of $\log K_F$ and n . The most important compound properties to predict $\log K_F$ were the degree of dissociation (A^- %), the pH-dependent hydrophobicity parameter $\log D_{\text{OW}}$, and the Abraham parameters for polarizability (S), H-bond basicity (B), and molar volume (V). The sensitivity of the predictions of $\log K_F$ to sorbent and sorbate properties was similar, whereas the prediction of n was largely driven (>80%) by the properties of the sorbent. Thus, sorption was driven by interactions with specific sorption sites,

which were consumed with increasing sorbent loading. Furthermore, the importance of SSA, H/C, and S indicated that π - π electron donor-acceptor interactions are a driving mechanism of sorption for negatively charged and polar compounds, as also reported in the literature.^{7,9}

3.3. Predicting Sorption of Cations and Zwitterions.

The same deep learning approach used for negatively charged and polar compounds was applied to compounds containing a positive charge. Therefore, the input layer was extended for an additional parameter that accounted for the abundance (%) of positively charged species, resulting in a total of 13 input parameters. The neural-network-based predictions of $\log K_F$ and n again yielded very accurate predictions over a wide working range of input parameters, as shown in Table 2 and Figure 4. Because of the smaller size of the training data set, the model's working range was smaller than for anions and polar compounds (see Tables 1 and 2). Similar to the predictions for anions and polar compounds, n was associated with higher prediction errors, likewise explained by the high concentration dependence of sorption nonlinearity (see Section 3.2).

To validate the predictions, we again randomly excluded 5% of the data lines (6 lines, see Table S4 in the Supporting Information) from the data set prior to neural network training. The results for these independent data confirmed the good predictions for both K_F and n for compounds containing a positive charge (Figure 5). However, the training data set was much smaller for this model than for the model presented in Section 3.2, and a larger body of literature will likely further increase the accuracy and applicability range of the model.

The calculation of the variance-based GSA was similar to that for anions and polar compounds. The importance of single input parameters for the prediction of $\log K_F$ and n was more evenly distributed (Figure 6), indicating that no single sorption process describable by these parameters was responsible for driving the sorption of compounds containing a positive charge. This is in good agreement with the literature, in which prediction of the sorption of compounds with a positive charge is often viewed as more challenging than is the case for negatively charged compounds.^{7,8} The dipolarity/polarizability S was the only sorbate parameter with little to no significance for the sorption of compounds with a positive charge. In contrast, S was a sorbate property of high importance for predicting the sorption of polar and negatively charged compounds. This indicates that π electron donor-acceptor interactions are generally not the drivers of the sorption of these compounds. Instead, the amount of ionized positively charged species was an important sorbate parameter for prediction, indicating that electrostatic attraction contributed substantially to sorption. Compounds containing a positive charge therefore exhibit a very distinct sorption behavior that is in stark contrast to the behavior of other organic compounds. Untangling of this distinct behavior to further improve predictive models and enable the production of sorbents tailored for cations and zwitterions is an important challenge for future research. In these studies, additional sorbent parameters such as cation exchange capacity should be considered during sorbent characterization because most of the published studies on the sorption of ionizable organic compounds have not reported cation- or anion-exchange capacities.

3.4. Potential Model Applications and Environmental Implications.

Prerequisites for the design of efficient water

purification systems or remediation strategies are easily accessible tools able to predict the sorption of emerging contaminants, which are often ionizable and polar compounds. To address this need, we made use of the available literature to develop two neural network-based models. Both performed excellently in predicting the sorption of organic anions, cations, and zwitterions as well as polar compounds to a wide range of carbonaceous materials. The first model was tailored to predict the sorption of polar and negatively charged contaminants and the second model that of compounds containing a positive charge, including zwitterions. To account for the concentration dependence of organic contaminant sorption to carbonaceous sorbent materials, both models can predict the Freundlich coefficient K_F and the exponent n that accounts for the concentration dependency of sorption. The provided models are able to cover a very wide range of sorption scenarios and will thus be useful for scientists and practitioners in the fields of water purification and remediation. To increase the accessibility of the models to those who are not familiar with computational environments, we provide a graphical user interface as [Supporting Information](#). To predict compounds and sorbent combinations with properties outside the range of the current version, the model can be trained with additional data, which will further improve its generalization and forecasting capabilities.

■ ASSOCIATED CONTENT

SI Supporting Information

The Supporting Information is available free of charge at <https://pubs.acs.org/doi/10.1021/acs.est.9b06287>.

All data used in this study, including the training datasets (XLSX)

“CFreupred” graphical user interface (ZIP)

■ AUTHOR INFORMATION

Corresponding Author

Thilo Hofmann – Department of Environmental Geosciences, Centre for Microbiology and Environmental Systems Science, University of Vienna, 1090 Wien, Austria; orcid.org/0000-0001-8929-6933; Phone: +43-1-4277-53320; Email: thilo.hofmann@univie.ac.at

Authors

Gabriel Sigmund – Department of Environmental Geosciences, Centre for Microbiology and Environmental Systems Science, University of Vienna, 1090 Wien, Austria; Agroscope, Environmental Analytics, CH-8046 Zurich, Switzerland; orcid.org/0000-0003-2068-0878

Mehdi Gharasoo – Department of Earth and Environmental Sciences, Ecohydrology, University of Waterloo, Waterloo, Ontario N2L 3G1, Canada

Thorsten Hüffer – Department of Environmental Geosciences, Centre for Microbiology and Environmental Systems Science, University of Vienna, 1090 Wien, Austria; orcid.org/0000-0002-5639-8789

Complete contact information is available at: <https://pubs.acs.org/doi/10.1021/acs.est.9b06287>

Notes

The authors declare no competing financial interest.

For further work based on these models, the MATLAB source codes can be provided upon request with the authors

■ ACKNOWLEDGMENTS

This study was partially funded by the Austrian Federal Ministry of Sustainability and Tourism (BMNT), management by Kommunalkredit Public Consulting GmbH (grant number B820017), the Canada First Research Excellence Fund (CFREF), and the Global Water Features (GWF) program. G.S. wrote part of this manuscript during his research stay at Nankai University, in Prof. Wei Chen's group, whose hospitality was greatly appreciated.

■ REFERENCES

- (1) Goss, K.-U.; Schwarzenbach, R. P. Linear Free Energy Relationships Used To Evaluate Equilibrium Partitioning of Organic Compounds. *Environ. Sci. Technol.* **2001**, *35*, 1–9.
- (2) Franco, A.; Ferranti, A.; Davidsen, C.; Trapp, S. An Unexpected Challenge: Ionizable Compounds in the REACH Chemical Space. *Int. J. Life Cycle Assess.* **2010**, *15*, 321–325.
- (3) Hüffer, T.; Endo, S.; Metzelder, F.; Schroth, S.; Schmidt, T. C. Prediction of Sorption of Aromatic and Aliphatic Organic Compounds by Carbon Nanotubes Using Poly-Parameter Linear Free-Energy Relationships. *Water Res.* **2014**, *59*, 295–303.
- (4) Shih, Y.-S.; Gschwend, P. M. Evaluating Activated Carbon-Water Sorption Coefficients of Organic Compounds Using a Linear Solvation Energy Relationship Approach and Sorbate Chemical Activities. *Environ. Sci. Technol.* **2009**, *43*, 851–857.
- (5) Lu, Z.; MacFarlane, J. K.; Gschwend, P. M. Adsorption of Organic Compounds to Diesel Soot: Frontal Analysis and Polyparameter Linear Free-Energy Relationship. *Environ. Sci. Technol.* **2016**, *50*, 285–293.
- (6) Endo, S.; Goss, K.-U. Applications of Polyparameter Linear Free Energy Relationships in Environmental Chemistry. *Environ. Sci. Technol.* **2014**, *48*, 12477–12491.
- (7) Kah, M.; Sigmund, G.; Xiao, F.; Hofmann, T. Sorption of Ionizable and Ionic Organic Compounds to Biochar, Activated Carbon and Other Carbonaceous Materials. *Water Res.* **2017**, *124*, 673–692.
- (8) European Centre for Ecotoxicology and Toxicology of Chemicals (ECETOC). *Environmental Exposure Assessment of Ionizable Organic Compounds*. Technical Report No. 123, 2013.
- (9) Pignatello, J. J.; Mitch, W. A.; Xu, W. Activity and Reactivity of Pyrogenic Carbonaceous Matter toward Organic Compounds. *Environ. Sci. Technol.* **2017**, *51*, 8893–8908.
- (10) Schenzel, J.; Goss, K.-U.; Schwarzenbach, R. P.; Bucheli, T. D.; Droge, S. T. J. Experimentally Determined Soil Organic Matter-Water Sorption Coefficients for Different Classes of Natural Toxins and Comparison with Estimated Numbers. *Environ. Sci. Technol.* **2012**, *46*, 6118–6126.
- (11) Sigmund, G.; Sun, H.; Hofmann, T.; Kah, M. Predicting the Sorption of Aromatic Acids to Noncarbonized and Carbonized Sorbents. *Environ. Sci. Technol.* **2016**, *50*, 3641–3648.
- (12) Sigmund, G.; Hüffer, T.; Hofmann, T.; Kah, M. Biochar Total Surface Area and Total Pore Volume Determined by N₂ and CO₂ Physisorption Are Strongly Influenced by Degassing Temperature. *Sci. Total Environ.* **2017**, *580*, 770–775.
- (13) Freundlich, H. Über die Adsorption in Lösungen. *Z. Phys. Chem.* **1907**, *57U*, 385.
- (14) Chingombe, P.; Saha, B.; Wakeman, R. J. Effect of Surface Modification of an Engineered Activated Carbon on the Sorption of 2,4-Dichlorophenoxy Acetic Acid and Benazolin from Water. *J. Colloid Interface Sci.* **2006**, *297*, 434–442.
- (15) Chen, W.; Duan, L.; Zhu, D. Adsorption of Polar and Nonpolar Organic Chemicals to Carbon Nanotubes. *Environ. Sci. Technol.* **2007**, *41*, 8295–8300.

- (16) Wang, S.; Tzou, Y.; Lu, Y.; Sheng, G. Removal of 3-Chlorophenol from Water Using Rice-Straw-Based Carbon. *J. Hazard. Mater.* **2007**, *147*, 313–318.
- (17) Chen, W.; Duan, L.; Wang, L.; Zhu, D. Adsorption of Hydroxyl- and Amino-Substituted Aromatics to Carbon Nanotubes. *Environ. Sci. Technol.* **2008**, *42*, 6862–6868.
- (18) Lin, D.; Xing, B. Adsorption of Phenolic Compounds by Carbon Nanotubes: Role of Aromaticity and Substitution of Hydroxyl Groups. *Environ. Sci. Technol.* **2008**, *42*, 7254–7259.
- (19) Chen, B.; Zhou, D.; Zhu, L. Transitional Adsorption and Partition of Nonpolar and Polar Aromatic Contaminants by Biochars of Pine Needles with Different Pyrolytic Temperatures. *Environ. Sci. Technol.* **2008**, *42*, 5137–5143.
- (20) Ji, L.; Liu, F.; Xu, Z.; Zheng, S.; Zhu, D. Adsorption of Pharmaceutical Antibiotics on Template-Synthesized Ordered Micro- and Mesoporous Carbons. *Environ. Sci. Technol.* **2010**, *44*, 3116–3122.
- (21) Wang, L.; Zhu, D.; Duan, L.; Chen, W. Adsorption of Single-Ringed N- and S-Heterocyclic Aromatics on Carbon Nanotubes. *Carbon* **2010**, *48*, 3906–3915.
- (22) Ji, L.; Chen, W.; Bi, J.; Zheng, S.; Xu, Z.; Zhu, D.; Alvarez, P. J. Adsorption of Tetracycline on Single-Walled and Multi-Walled Carbon Nanotubes as Affected by Aqueous Solution Chemistry. *Environ. Toxicol. Chem.* **2010**, *29*, 2713–2719.
- (23) Sheng, G. D.; Shao, D. D.; Ren, X. M.; Wang, X. Q.; Li, J. X.; Chen, Y. X.; Wang, X. K. Kinetics and Thermodynamics of Adsorption of Ionizable Aromatic Compounds from Aqueous Solutions by As-Prepared and Oxidized Multiwalled Carbon Nanotubes. *J. Hazard. Mater.* **2010**, *178*, 505–516.
- (24) Wang, Z.; Yu, X.; Pan, B.; Xing, B. Norfloxacin Sorption and Its Thermodynamics on Surface-Modified Carbon Nanotubes. *Environ. Sci. Technol.* **2010**, *44*, 978–984.
- (25) Uchimiya, M.; Wartelle, L. H.; Lima, I. M.; Klasson, K. T. Sorption of Deisopropylatrazine on Broiler Litter Biochars. *J. Agric. Food Chem.* **2010**, *58*, 12350–12356.
- (26) Zheng, W.; Guo, M.; Chow, T.; Bennett, D. N.; Rajagopalan, N. Sorption Properties of Greenwaste Biochar for Two Triazine Pesticides. *J. Hazard. Mater.* **2010**, *181*, 121–126.
- (27) Li, X.; Zhao, H.; Quan, X.; Chen, S.; Zhang, Y.; Yu, H. Adsorption of Ionizable Organic Contaminants on Multi-Walled Carbon Nanotubes with Different Oxygen Contents. *J. Hazard. Mater.* **2011**, *186*, 407–415.
- (28) Sun, K.; Ro, K.; Guo, M.; Novak, J.; Mashayekhi, H.; Xing, B. Sorption of bisphenol A, 17 α -ethinyl estradiol and phenanthrene on thermally and hydrothermally produced biochars. *Bioresour. Technol.* **2011**, *102*, 5757–5763.
- (29) Sun, K.; Keiluweit, M.; Kleber, M.; Pan, Z.; Xing, B. Sorption of Fluorinated Herbicides to Plant Biomass-Derived Biochars as a Function of Molecular Structure. *Bioresour. Technol.* **2011**, *102*, 9897–9903.
- (30) Zhang, G.; Zhang, Q.; Sun, K.; Liu, X.; Zheng, W.; Zhao, Y. Sorption of Simazine to Corn Straw Biochars Prepared at Different Pyrolytic Temperatures. *Environ. Pollut.* **2011**, *159*, 2594–2601.
- (31) Sun, K.; Zhang, Z.; Gao, B.; Wang, Z.; Xu, D.; Jin, J.; Liu, X. Adsorption of Diuron, Fluridone and Norflurazon on Single-Walled and Multi-Walled Carbon Nanotubes. *Sci. Total Environ.* **2012**, *439*, 1–7.
- (32) Li, Y.; Du, Q.; Liu, T.; Sun, J.; Jiao, Y.; Xia, Y.; Xia, L.; Wang, Z.; Zhang, W.; Wang, K.; Zhu, H.; Wu, D. Equilibrium, Kinetic and Thermodynamic Studies on the Adsorption of Phenol onto Graphene. *Mater. Res. Bull.* **2012**, *47*, 1898–1904.
- (33) Liao, P.; Yuan, S.; Zhang, W.; Tong, M.; Wang, K. Mechanistic Aspects of Nitrogen-Heterocyclic Compound Adsorption on Bamboo Charcoal. *J. Colloid Interface Sci.* **2012**, *382*, 74–81.
- (34) Liu, P.; Liu, W.-J.; Jiang, H.; Chen, J.-J.; Li, W.-W.; Yu, H.-Q. Modification of Bio-Char Derived from Fast Pyrolysis of Biomass and Its Application in Removal of Tetracycline from Aqueous Solution. *Bioresour. Technol.* **2012**, *121*, 235–240.
- (35) Sun, K.; Jin, J.; Keiluweit, M.; Kleber, M.; Wang, Z.; Pan, Z.; Xing, B. Polar and Aliphatic Domains Regulate Sorption of Phthalic Acid Esters (PAEs) to Biochars. *Bioresour. Technol.* **2012**, *118*, 120–127.
- (36) Lü, J.; Li, J.; Li, Y.; Chen, B.; Bao, Z. Use of Rice Straw Biochar Simultaneously as the Sustained Release Carrier of Herbicides and Soil Amendment for Their Reduced Leaching. *J. Agric. Food Chem.* **2012**, *60*, 6463–6470.
- (37) Zhang, P.; Sun, H.; Yu, L.; Sun, T. Adsorption and Catalytic Hydrolysis of Carbaryl and Atrazine on Pig Manure-Derived Biochars: Impact of Structural Properties of Biochars. *J. Hazard. Mater.* **2013**, *244–245*, 217–224.
- (38) Liao, P.; Yuan, S.; Xie, W.; Zhang, W.; Tong, M.; Wang, K. Adsorption of Nitrogen-Heterocyclic Compounds on Bamboo Charcoal: Kinetics, Thermodynamics, and Microwave Regeneration. *J. Colloid Interface Sci.* **2013**, *390*, 189–195.
- (39) Wang, C.; Li, H.; Liao, S.; Zheng, H.; Wang, Z.; Pan, B.; Xing, B. Co-adsorption, Desorption Hysteresis and Sorption Thermodynamics of Sulfamethoxazole and Carbamazepine on Graphene Oxide and Graphite. *Carbon* **2013**, *65*, 243–251.
- (40) Li, J.; Li, Y.; Wu, M.; Zhang, Z.; Lü, J. Effectiveness of Low-Temperature Biochar in Controlling the Release and Leaching of Herbicides in Soil. *Plant Soil* **2013**, *370*, 333–344.
- (41) Tatarková, V.; Hiller, E.; Vaculík, M. Impact of Wheat Straw Biochar Addition to Soil on the Sorption, Leaching, Dissipation of the Herbicide (4-Chloro-2-Methylphenoxy)Acetic Acid and the Growth of Sunflower (*Helianthus Annuus* L.). *Ecotoxicol. Environ. Saf.* **2013**, *92*, 215–221.
- (42) Li, X.; Pignatello, J. J.; Wang, Y.; Xing, B. New Insight into Adsorption Mechanism of Ionizable Compounds on Carbon Nanotubes. *Environ. Sci. Technol.* **2013**, *47*, 8334–8341.
- (43) Zhao, X.; Ouyang, W.; Hao, F.; Lin, C.; Wang, F.; Han, S.; Geng, X. Properties Comparison of Biochars from Corn Straw with Different Pretreatment and Sorption Behaviour of Atrazine. *Bioresour. Technol.* **2013**, *147*, 338–344.
- (44) Han, X.; Liang, C.-F.; Li, T.-q.; Wang, K.; Huang, H.-g.; Yang, X.-e. Simultaneous Removal of Cadmium and Sulfamethoxazole from Aqueous Solution by Rice Straw Biochar. *J. Zhejiang Univ., Sci., B* **2013**, *14*, 640–649.
- (45) Zheng, H.; Wang, Z.; Zhao, J.; Herbert, S.; Xing, B. Sorption of Antibiotic Sulfamethoxazole Varies with Biochars Produced at Different Temperatures. *Environ. Pollut.* **2013**, *181*, 60–67.
- (46) Wu, M.; Pan, B.; Zhang, D.; Xiao, D.; Li, H.; Wang, C.; Ning, P. The Sorption of Organic Contaminants on Biochars Derived from Sediments with High Organic Carbon Content. *Chemosphere* **2013**, *90*, 782–788.
- (47) Kearns, J. P.; Wellborn, L. S.; Summers, R. S.; Knappe, D. R. U. 2,4-D Adsorption to Biochars: Effect of Preparation Conditions on Equilibrium Adsorption Capacity and Comparison with Commercial Activated Carbon Literature Data. *Water Res.* **2014**, *62*, 20–28.
- (48) Zhu, X.; Liu, Y.; Zhou, C.; Luo, G.; Zhang, S.; Chen, J. A Novel Porous Carbon Derived from Hydrothermal Carbon for Efficient Adsorption of Tetracycline. *Carbon* **2014**, *77*, 627–636.
- (49) Lian, F.; Sun, B.; Song, Z.; Zhu, L.; Qi, X.; Xing, B. Physicochemical Properties of Herb-Residue Biochar and Its Sorption to Ionizable Antibiotic Sulfamethoxazole. *Chem. Eng. J.* **2014**, *248*, 128–134.
- (50) Rajapaksha, A. U.; Vithanage, M.; Zhang, M.; Ahmad, M.; Mohan, D.; Chang, S. X.; Ok, Y. S. Pyrolysis Condition Affected Sulfamethazine Sorption by Tea Waste Biochars. *Bioresour. Technol.* **2014**, *166*, 303–308.
- (51) Chen, C.; Zhou, W.; Lin, D. Sorption Characteristics of N-Nitrosodimethylamine onto Biochar from Aqueous Solution. *Bioresour. Technol.* **2015**, *179*, 359–366.
- (52) Zhang, C.; Lai, C.; Zeng, G.; Huang, D.; Yang, C.; Wang, Y.; Zhou, Y.; Cheng, M. Efficacy of Carbonaceous Nanocomposites for Sorbing Ionizable Antibiotic Sulfamethazine from Aqueous Solution. *Water Res.* **2016**, *95*, 103–112.

(53) Ren, X.; Sun, H.; Wang, F.; Cao, F. The Changes in Biochar Properties and Sorption Capacities after Being Cultured with Wheat for 3 Months. *Chemosphere* **2016**, *144*, 2257–2263.

(54) Sun, K.; Kang, M.; Ro, K. S.; Libra, J. A.; Zhao, Y.; Xing, B. Variation in Sorption of Propiconazole with Biochars: The Effect of Temperature, Mineral, Molecular Structure, and Nano-Porosity. *Chemosphere* **2016**, *142*, 56–63.

(55) Zhang, F.; Li, Y.; Zhang, G.; Li, W.; Yang, L. The Importance of Nano-Porosity in the Stalk-Derived Biochar to the Sorption of 17 β -Estradiol and Retention of It in the Greenhouse Soil. *Environ. Sci. Pollut. Res.* **2017**, *24*, 9575–9584.

(56) Luo, J.; Li, X.; Ge, C.; Müller, K.; Yu, H.; Huang, P.; Li, J.; Tsang, D. C. W.; Bolan, N. S.; Rinklebe, J.; et al. Sorption of Norfloxacin, Sulfamerazine and Oxytetracycline by KOH-Modified Biochar under Single and Ternary Systems. *Bioresour. Technol.* **2018**, *263*, 385–392.

(57) Liu, Y.; Sohi, S. P.; Jing, F.; Chen, J. Oxidative Ageing Induces Change in the Functionality of Biochar and Hydrochar: Mechanistic Insights from Sorption of Atrazine. *Environ. Pollut.* **2019**, *249*, 1002–1010.

(58) Jia, M.; Wang, F.; Bian, Y.; Stedtfeld, R. D.; Liu, G.; Yu, J.; Jiang, X. Sorption of Sulfamethazine to Biochars as Affected by Dissolved Organic Matters of Different Origin. *Bioresour. Technol.* **2018**, *248*, 36–43.

(59) Chang, Z.; Tian, L.; Wu, M.; Dong, X.; Peng, J.; Pan, B. Molecular Markers of Benzene Polycarboxylic Acids in Describing Biochar Physicochemical Properties and Sorption Characteristics. *Environ. Pollut.* **2018**, *237*, 541–548.

(60) MacKay, D. J. C. Bayesian Interpolation. *Neural Comput.* **1992**, *4*, 415–447.

(61) Dan Foresee, F.; Hagan, M. T. Gauss-Newton Approximation to Bayesian Regularization. *Proceedings 1997 International Joint Conference Neural Networks*, 1997; pp 1930–1935.

(62) Sobol', I. M. Global Sensitivity Indices for Nonlinear Mathematical Models and Their Monte Carlo Estimates. *Math. Comput. Simulat.* **2001**, *55*, 271–280.

(63) Gharasoo, M.; Ehrl, B. N.; Cirpka, O. A.; Elsner, M. Modeling of Contaminant Biodegradation and Compound-Specific Isotope Fractionation in Chemostats at Low Dilution Rates. *Environ. Sci. Technol.* **2019**, *53*, 1186–1196.

(64) Sobol', I. M.; Levitan, Y. L. On the Use of Variance Reducing Multipliers in Monte Carlo Computations of a Global Sensitivity Index. *Comput. Phys. Commun.* **1999**, *117*, 52–61.

(65) Gharasoo, M.; Thullner, M.; Elsner, M. Introduction of a New Platform for Parameter Estimation of Kinetically Complex Environmental Systems. *Environ. Model. Software* **2017**, *98*, 12–20.

(66) Gharasoo, M.; Wietzke, L. M.; Knorr, B.; Bakkour, R.; Elsner, M.; Stumpp, C. A Robust Optimization Technique for Analysis of Multi-Tracer Experiments. *J. Contam. Hydrol.* **2019**, *224*, 103481.

(67) Hale, S. E.; Arp, H. P. H.; Kupryianchyk, D.; Cornelissen, G. A Synthesis of Parameters Related to the Binding of Neutral Organic Compounds to Charcoal. *Chemosphere* **2016**, *144*, 65–74.

(68) Burg, P.; Abraham, M. H.; Cagniant, D. Methods of Determining Polar and Non-Polar Sites on Carbonaceous Adsorbents. The Contribution of the Linear Solvation Energy Relationship Approach. *Carbon* **2003**, *41*, 867–879.

(69) Ulrich, N.; Endo, S.; Brown, T. N.; Watanabe, N.; Bronner, G.; Abraham, M. H.; Goss, K.-U. *UFZ-LSER Database v 3.2* <http://www.ufz.de/lserd>.